Copolymer Fingerprints of Polystyrene-*block*-polyisoprene by MALDI-ToF-MS

Robin X. E. Willemse, Bastiaan B. P. Staal, Ellen H. D. Donkers, and Alex M. van Herk*

Laboratory of Polymer Chemistry, Department of Chemical Engineering, Eindhoven University of Technology, P.O. Box 513, 5600 MB, Eindhoven, The Netherlands

Received March 17, 2004; Revised Manuscript Received May 24, 2004

ABSTRACT: MALDI-ToF-MS mass spectra of copolymers contain a lot of information on both chain length distribution (CLD) and chemical composition distribution (CCD). In this paper an approach for extracting detailed information from a MALDI-ToF-MS mass spectrum is presented that enables the study of microstructure for copolymers. More specifically, this paper is dealing with a polystyrene-*block*-polyisoprene copolymer, in which the growth of the second block is followed with MALDI-ToF-MS as a function of conversion. The technique is compared to ^{1}H NMR for the evaluation of average chemical compositions, revealing that ionization efficiencies do not influence the obtained mass spectra. It is shown that MALDI-ToF-MS can extract detailed information on the chain length distributions (CLDs) for both polystyrene and polyisoprene blocks. Using random coupling statistics, it is shown that the proposed analysis yields results with a high accuracy.

Introduction

With the introduction of controlled polymerization techniques in the 1950s, scientists succeeded in creating (co)polymers having predefined narrow chain length distributions (CLD). The type of control gained by these procedures led to new polymeric structures with different chemical composition distributions (CCD) of which block copolymers or gradient copolymers are mere examples. Because of the increased complexity of these types of copolymers, new routes had to be developed for their analysis.

Characterization of copolymers comprises not only the analysis of CLDs but also the analysis of CCDs. To accomplish this, usually a combination of different techniques is applied. In the literature examples are found where size exclusion chromatography (SEC) is used to accomplish separation by molecular weight, after which MALDI-ToF-MS is used for the characterization of molecular weight and NMR to determine the chemical composition.[1−3] Another technique that is gaining interest for the analysis of copolymer systems comprises two-dimensional liquid chromatography where usually in the first dimension liquid chromatography is used in which the separation is based on chemical composition and SEC in the second dimension to accomplish separation on molar masses.[4−14]

A very important technique for the analysis of polymers in general and more specifically copolymers is matrix-assisted laser desorption ionization time-of-flight mass spectrometry (MALDI-ToF-MS). It has been successfully applied in combination with SEC analysis to provide off-line calibration for homo- and copolymers, leading to more accurate calibration curves even up to very high masses.[15−25] The technique itself can, however, also be used to combine a CLD and CCD analysis in one go, although the mass range applicable for this analysis is limited. One of the first examples of this combined analysis can be found in the work of Wilczek-Vera et al.,[26−28] although their analysis was limited to lower masses due to the lower resolution of the measurements. (Measurements were carried out in the linear mode.) Their work was later on followed up by Suddaby et al.,[29] Van Rooij et al.,[30] and Suen et al.[31] although, strictly speaking, the technique used by Van Rooij et al. is not a MALDI-ToF-MS technique.

The goal of this article is to show that an analysis based on the concepts by Wilczek-Vera et al.[26−28] can be applied to investigate the microstructure of copolymer samples, provided that the analysis is carried out in the reflector mode. The proposed procedure will be illustrated for a polystyrene-*block*-polyisoprene copolymer and compared to ^{1}H NMR. For this particular system, an additional complicating factor is the small mass difference between (multiples of) comonomers, which results in overlapping isotopic patterns. However, it will be shown that this overlapping of peaks has no observable effect on the obtained results. Finally, random coupling statistics[26−28,30] are applied to study the robustness of the method.

Experimental Section

Polymerization. The polystyrene-*block*-polyisoprene copolymer was prepared by anionic polymerization using *sec*-butyllithium (Acros, 1.3 M solution in cyclohexane/hexane (92/8)) as the initiator. Reactions were carried out in a 2 L stainless steel autoclave reactor under a nitrogen atmosphere using cyclohexane (VWR, high purity) as a solvent. Monomers and solvent were passed over an activated alumina column prior to polymerization. The autoclave reactor was loaded with 1 kg of cyclohexane and heated to 40 °C. For the first block 50 g of styrene (VWR, 99%) was added followed by 25 mL of 1 M *sec*-butyllithium in cyclohexane. Styrene polymerization was allowed to reach full conversion (reaction time ± 80 min), after which a sample was taken that was terminated by quenching in an excess of methanol. For the second block 50 g of isoprene (Mitsui & Co.) was added. Samples were withdrawn from the reaction mixture after approximately 4, 10, 20, and 120 min (corresponding to approximately 25, 50, 75, and 100% conversion of the isoprene monomer) and quenched in excess methanol.

Analysis. MALDI-ToF-MS analysis was carried out on a Voyager DE-STR from Applied Biosystems. The matrix used for the analysis is *trans*-2-[3-(4-*tert*-butylphenyl)-2-methyl-2-

* Corresponding author. E-mail A.M.v.Herk@tue.nl.

10.1021/ma049471m CCC: $27.50
Published on Web 06/29/2004

propenylidene]malononitrile (DCTB) which was synthesized according to literature procedures.[32] The matrix was dissolved in THF at a concentration of 40 mg mL^{-1}. Silver trifluoracetate (Aldrich, 98%) was used as cationization agent and was added to THF at typical concentrations of 1 mg mL^{-1}. The polymer was dissolved in THF at approximately 2 mg mL^{-1}. In a typical MALDI-ToF-MS experiment the matrix, salt, and polymer solution were premixed in a ratio of 10:1:5. The premixed solutions were hand-spotted on the target well and left to dry. All mass spectra were recorded in the reflector mode and are the result of approximately 5000 individual laser shots. Mass spectra were baseline corrected with the advanced baseline correction mode from the Data Explorer software from Applied Biosystems. For a correct interpretation of MALDI-ToF-MS mass spectra, isotopic patterns of single polymer chains need to be integrated in the mass domain.[33] This integration was carried out for sample I (homopolymer of polystyrene). Because of the complexity of copolymer mass spectra, this integration procedure cannot be applied, and therefore these mass spectra were analyzed using a homemade program[34] written in Visual Basic 6.0. This program needs the molecular formulas of the repeat units, end groups, and cation as an input for a full mass spectral analysis.

^{1}H NMR was carried out to determine average copolymer compositions. ^{1}H NMR spectra were recorded with a Varian 400 MHz spectrometer at 298 K, using $CDCl_3$ as a solvent.

Results and Discussion

Advanced MALDI-ToF-MS Analysis. The mass for single charged copolymers can be calculated by the general formula

$$m_{\mathrm{th}} = n_i M_i + m_j M_j + E_{\mathrm{I}} + E_{\mathrm{II}} + M^+ \qquad (1)$$

which relates the mass of the copolymer to the chemical composition (n_i and m_j) of the monomeric units (M_i and M_j) and the masses of the end groups (E_{I} and/or E_{II}) plus cationization agent (M^+). Since copolymers have a distribution over the chain length as well as the chemical composition, the obtained mass spectra can be very complicated to interpret. Access to a method that allows an easy interpretation of the MALDI-ToF-MS mass spectra is therefore very important and can be carried out in a relatively simple way.

Let there be a matrix consisting of n_i rows and m_j columns. With knowledge of the different end groups (E_{I} and E_{II}) and the cationization agent (M^+), each position in the matrix, (n_i, m_j), corresponds to a theoretical mass of single charged copolymers, m_{th}, which can be calculated using eq 1.

With the inequality

$$|m_{\mathrm{exp}} - m_{\mathrm{th}}| \leq \frac{\Delta m}{2} \qquad (2)$$

where Δm represents the accuracy (usually in the range 1−2 g mol^{-1}); the mass peak in a MALDI-ToF-MS spectrum with the highest intensity ($I_{i,j}$) that still falls within the accuracy (eq 2) can be assigned to a position in the matrix at the location (n_i, m_j).

Two additional phenomena have to be taken into account before processing of the data can occur. First of all, the method that is proposed only takes the most abundant isotope into account. With masses increasing, the contribution of the most abundant isotope with respect to the isotopic pattern decreases, and a correction for this is necessary. Second, the proposed method uses the peak intensity for the calculations, but it is not the peak intensity but the area beneath an isotope that relates to the number of polymeric chains. For MALDI-ToF-MS mass spectra of copolymer species, it is very difficult to integrate these individual isotopes, since isotopic patterns are becoming broader with an increase in mass and overlap between different isotopic distributions can occur.

	m_0	...	m_j	...	m_n
n_0	$I_{(0,0)} \cdot cf_{0,0}$	...	$I_{(0,j)} \cdot cf_{0,j}$	...	$I_{(0,n)} \cdot cf_{0,n}$
...	...	...	...	...	...
n_i	$I_{(i,0)} \cdot cf_{i,0}$	...	$I_{(i,j)} \cdot cf_{i,j}$	...	$I_{(i,n)} \cdot cf_{i,n}$
...	...	...	...	...	...
n_n	$I_{(n,0)} \cdot cf_{n,0}$	...	$I_{(n,j)} \cdot cf_{n,j}$	...	$I_{(n,n)} \cdot cf_{n,n}$

Figure 1. Schematic representation of a MALDI-ToF-MS spectrum in a matrix.

To overcome both of these phenomena, a correction factor ($cf_{i,j}$) is introduced that relates the peak height ($I_{i,j}$) of the most intense isotope of a polymeric species to the theoretical area underneath the isotopic distribution (see Appendix A). The peak height subsequently has to be multiplied with this correction factor, $cf_{i,j}$. Note that this correction factor does not take the overlap between neighboring peaks into account. Finally, the resulting matrix is normalized.

After analysis of the copolymer mass spectrum, this normalized matrix can be represented either as a three-dimensional graph[26−29] or as a two-dimensional contour plot.[30] The latter representation is favorable since two-dimensional plots are easier to interpret as they result in a so-called "fingerprint" of the copolymer under investigation.

Multiple Peak Assignment. One additional problem in analyzing MALDI-ToF-MS mass spectra is that sometimes copolymer masses can be assigned by different number combinations of the two monomer repeat units.

This is best illustrated in the following way. Let there be a mass peak that can be assigned to a matrix position (n_{A},m_{B}), corresponding to n_{A} units of monomer A and m_{B} units of monomer B. By exchanging Δn_{A} units of monomer A for Δm_{B} units of monomer B, the same mass peak can also be assigned to the position ($n_{\mathrm{A}} - \Delta n_{\mathrm{A}}$, $m_{\mathrm{B}} + \Delta m_{\mathrm{B}}$) in the matrix. Wilczek-Vera et al.[26] have also addressed this problem, and a simple way to calculate the number of units Δn_{A} and Δm_{B} that can be replaced for one another has been proposed as

$$\frac{\Delta n_{\mathrm{A}}}{\Delta m_{\mathrm{B}}} = \frac{M_{\mathrm{B}}}{M_{\mathrm{A}}} \qquad (3)$$

in which Δn_{A} and Δm_{B} are related to the masses of the repeat units M_{A} and M_{B}. The problem of multiple peak assignment therefore requires additional knowledge of the copolymer under investigation in order to clean the obtained matrix. This additional information can be obtained from other techniques such as ^{1}H NMR or, as is the case in this article, from the analysis of the first block in a block copolymer. (See Supporting Information for an example of this multiple peak assignment problem.)

Polystyrene-*block*-polyisoprene. The five samples that were withdrawn from the block copolymer synthesis at different reaction times were analyzed with MALDI-ToF-MS. Figure 2 only includes the first, third,

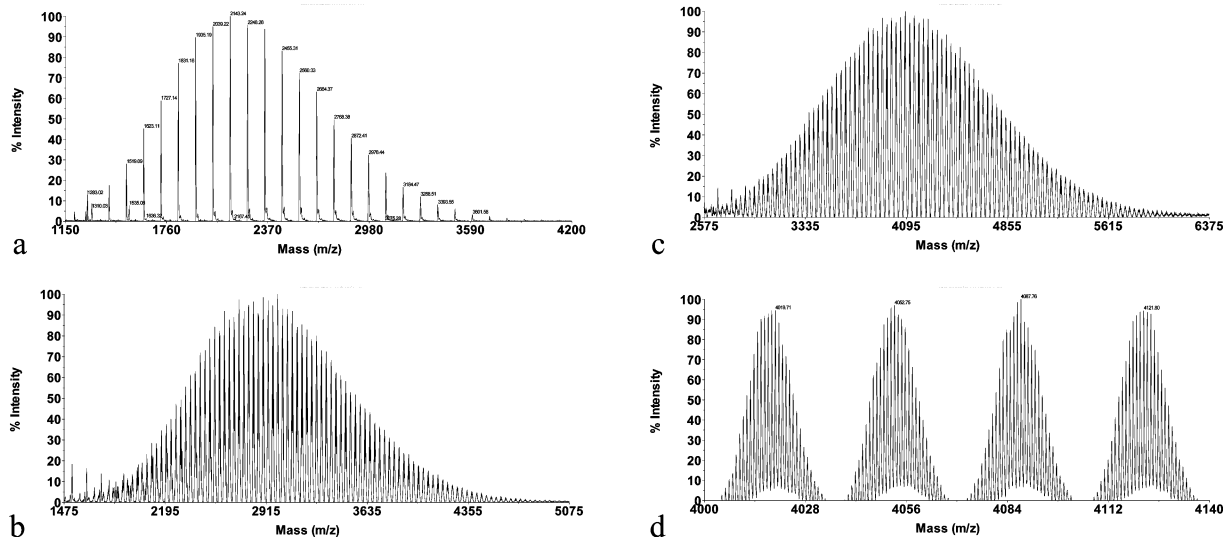

Figure 2. (a−c) MALDI-ToF-MS mass spectra of the system polystyrene-*block*-polyisoprene after 0%, 50%, and 100% conversion of the isoprene monomer and (d) an enlargement of (c) between 4000 and 4140 g·mol^{-1}. MALDI-ToF-MS mass spectra after approximately 25% and 75% conversion of the isoprene monomer are included in the Supporting Information.

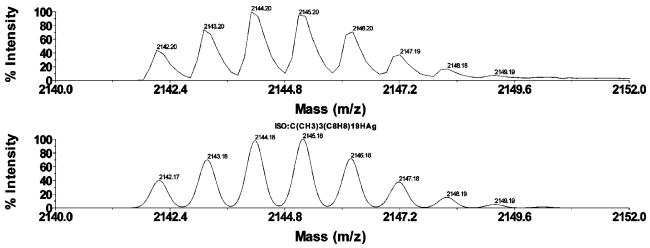

Figure 3. Comparison between the isotopic patterns of sample I (upper spectrum) and the theoretical isotopic distribution (lower spectrum) in the mass range of 2140 and 2152 g mol^{-1}, demonstrating a clear match between the two patterns.

and fifth sample whereas samples two and four are included in the Supporting Information. Figure 2a comprises the polystyrene block after 100% conversion of styrene, and as shown in Figure 3, there is a clear match between the masses of the peaks when comparing the theoretical isotopic pattern with the measured isotopic pattern.

Figure 2b,c comprises the polystyrene-*block*-polyisoprene samples after approximately 50 and 100% conversion of the isoprene monomer. Figure 2d is an enlargement of Figure 2c, clearly demonstrating that the isotopic patterns are well resolved. The complicated isotopic pattern arises due to the difference of only 4 g mol^{-1} between 3 isoprene units and 2 styrene units combined with the isotopic pattern of the silver cation.

As discussed before, each polymeric chain of the polystyrene-*block*-polyisoprene copolymer consists of one secondary butyl end group (E_I = 57.115 g mol^{-1}), one hydrogen end group (E_{II} = 1.008 g mol^{-1}), n_{St} units of styrene (M_{St} = 104.15 g mol^{-1}), and $n_{isoprene}$ units of isoprene ($M_{isoprene}$ = 68.12 g mol^{-1}). With this knowledge in mind the copolymer fingerprints were constructed with the use of eq 2 using an accuracy of 1.5 g mol^{-1}, resulting in the copolymer fingerprints as displayed in Figure 4a−d. In the Supporting Information an example is given of Figure 4d where it can be clearly observed that multiple peak assignments lead to copolymer fingerprints at different locations. In this specific example the knowledge of the number-average degree of polymerization of the polystyrene block allows for an easy identification of the "true" copolymer fingerprint.

Examination of the copolymer fingerprints in Figure 4a−d gives a clear indication of the growth of the polyisoprene block. As expected the growth takes place only in the direction of the isoprene axis, whereas no apparent change is observed along the styrene axis.

A key issue in MALDI-ToF-MS analysis is the impact of discrimination effects due to mass differences and differences in ionization efficiency due to chemical composition differences. While it can be assumed that mass discrimination does not play a role as long as the polydispersity index of the sample is lower than 1.2,[35] differences in ionization efficiency may have its effect on the obtained results. A good example of this phenomenon is given by the work of Wilczek-Vera et al.[26] in which a discrepancy between the analysis of a poly(α-methylstyrene)-*block*-poly(4-vinylpyridine) by ^{1}H NMR and MALDI-ToF-MS was found. This example clearly illustrates that, although MALDI-ToF-MS in essence can result in reliable average chemical composition measurements, the results have to be interpreted with caution.

For the polystyrene-*block*-polyisoprene it can be assumed that mass discrimination does not play a role since the polydispersity index of the whole sample is lower than 1.2. A good way to see whether mass discrimination due to differences in ionization efficiencies play an important role is the comparison with an independent technique such as ^{1}H NMR. For this reason, the average compositions of the copolymer were calculated by both MALDI-ToF-MS with the use of eq 16 (Appendix B) and compared to ^{1}H NMR. The results of this are tabulated in Table 1, demonstrating a very good agreement between the two independent techniques. These results therefore confirm that differences in ionization efficiencies do not play a significant role in this specific system.

Individual Block Properties. One very obvious but important feature of Figure 4a−d is the observation that there is no change in the distribution of the polystyrene block. Since Figure 4a−d is only demonstrating the growth of the polyisoprene block, this by definition implies that the polystyrene distribution cannot change. A way to further investigate this is by the analysis of the individual block properties of the polystyrene and polyisoprene block, which can be evaluated from the

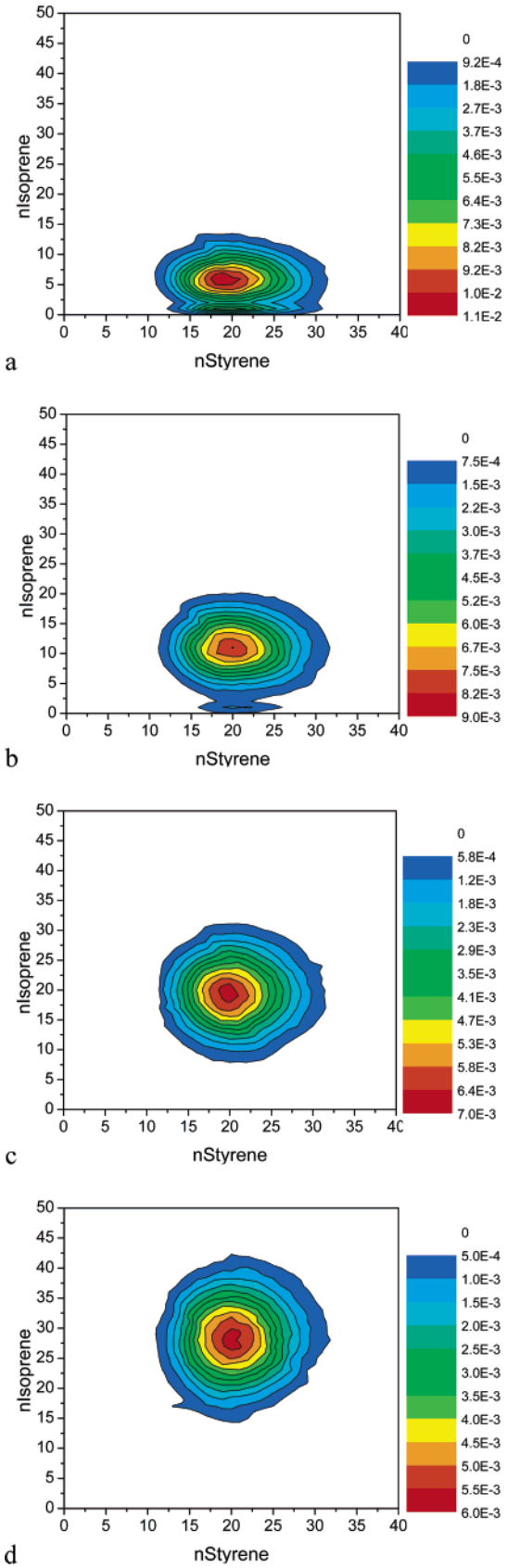

Figure 4. (a−d) Copolymer fingerprints of the system polystyrene-*block*-polyisoprene corresponding to approximately 25%, 50%, 75%, and 100% conversion of the isoprene monomer.

calculated copolymer fingerprints as has been demonstrated by Wilczek-Vera et al.[28] To obtain the individual block distribution of for example the polystyrene block, all intensities along the isoprene axis have to be summed according to

$$\Gamma^{St}(n_{St}) = \sum_{m_{isoprene}} (I_{n_{St},m_{isoprene}} cf_{n_{St},m_{isoprene}}) \qquad (4)$$

in which $\Gamma^{St}(n_{St})$ is the intensity for the individual polystyrene block distribution consisting of n_{St} units. These individual block distributions allow for a detailed investigation of the individual blocks. Figure 5a clearly demonstrates the normalized polystyrene block distributions for all four block samples compared to the original polystyrene distribution obtained from Figure 2a. It can be observed that there is an excellent match between the original polystyrene distribution (sample I, solid line) and the obtained individual block distributions (symbols) as was already indicated by the fingerprints. Table 2 tabulates the calculated individual block properties for both polystyrene and polyisoprene, further demonstrating that the polystyrene distributions for all five samples are nearly identical. This proves that the problem of overlapping isotopes does not play an important role in this specific example and can therefore be safely neglected.

Table 1. Average Composition of the Polystyrene-*block*-polyisoprene Samples As Measured by ^{1}H NMR and Calculated with the Use of Eq 16 (Appendix B)

sample	^{1}H NMR $F_{styrene}$	MALDI-ToF-MS $F_{styrene}$
II	0.79	0.77
III	0.67	0.66
IV	0.53	0.52
V	0.45	0.42

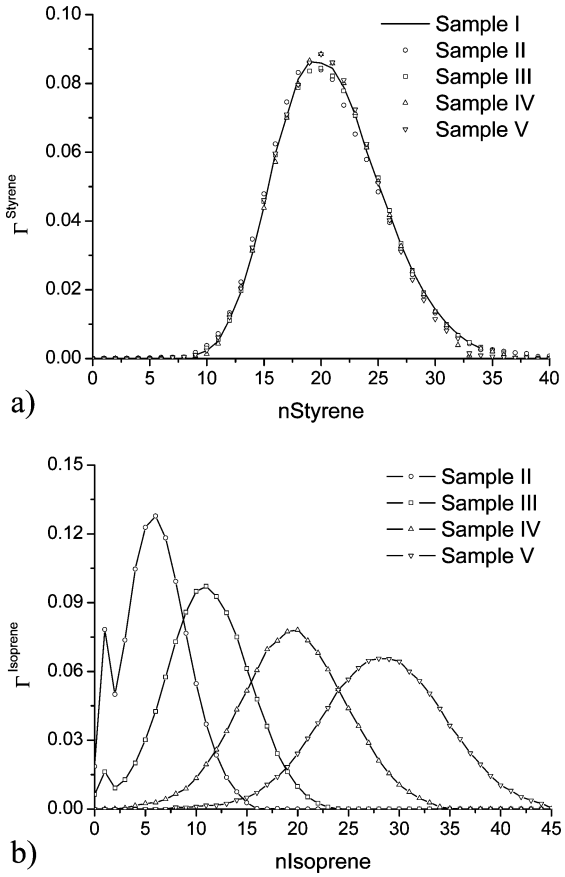

Figure 5. (a) Individual block distributions of polystyrene (symbols) compared to the original polystyrene block (solid line) and (b) the individual block distributions of the polyisoprene block.

Table 2. Individual Block Properties Calculated from the Individual Block Distributions Using the Equations As Provided in Appendix B

	polystyrene block			polyisoprene block		
sample	P_n	P_w	PDI	P_n	P_w	PDI
I	20.84	21.83	1.05			
II	20.73	21.90	1.06	6.02	7.65	1.27
III	20.89	21.93	1.05	11.00	12.60	1.15
IV	20.80	21.77	1.05	19.55	20.92	1.07
V	20.64	21.59	1.05	28.41	29.66	1.04

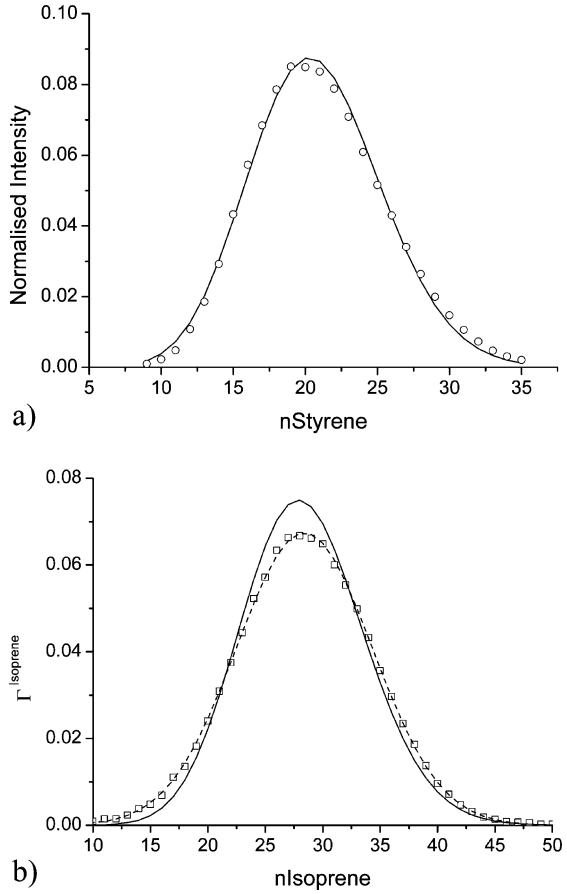

Figure 6. Comparison between (a) polystyrene block (sample I, ○) and the Poisson distribution (—, μ = 20.84) and (b) polyisoprene block (sample V, □) Poisson distribution (—, μ = 28.41) and Gauss distribution (- - -, μ = 28.41, σ = 5.92).

Figure 5b demonstrates the evolution of the polyisoprene block at different conversions of the second block. As seen from Table 2 with an increase of polymerization, the polydispersity index (PDI) of the polyisoprene block decreases as expected from a controlled polymerization process.

Individual Block Distributions. It is generally accepted that for anionic polymerizations the polymer growth can be described by a Poisson distribution as long as the rate of initiation is faster than the rate of propagation:[36]

$$X(i) = \frac{\mu^i e^{-\mu}}{i!} \tag{5}$$

where $X(i)$ is the number fraction of chains with chain length i and μ is the number-average degree of polymerization. A close look at Figure 6a demonstrates that the polystyrene block can indeed be described with the Poisson distribution. Comparison between sample 5 and the Poisson distribution (Figure 6b), however, reveals that the polyisoprene block cannot be described by the Poisson distribution because this distribution is too broad. For this reason a second distribution, the Gauss or normal distribution, was tested:

Table 3. Statistical Analysis of the Copolymer Mass Spectra by the Random Coupling Theory

sample	correlation coeff (r)	unexplained variance (%) ($1 - r^2$)
II	0.998	0.35
III	0.998	0.31
IV	0.998	0.43
V	0.998	0.33

$$X(i) = \frac{1}{\sigma\sqrt{2\pi}} e^{-((i-\mu)^2/2\sigma^2)} \tag{6}$$

where σ is the width of the distribution. Comparing the Gauss distribution with the polyisoprene distribution demonstrates a good fit with the Gauss distribution, indicating that the growth of the polyisoprene block is less controlled than that of the polystyrene block. The reason for this is already revealed at the lower conversions of the polyisoprene block when a closer look is taken at Figure 5b (samples II and III). It can be observed that for at least part of the chains the addition of the second isoprene unit is retarded. An explanation for this phenomenon may be related to the possibility of head-to-tail addition vs head-to-head addition that is known to occur in isoprene polymerization.[36] If these two different types of addition occur with different reaction rates due to a different stabilization of the anion, the anionic polymerization, which is normally governed by a Poisson distribution, is less controlled; i.e., broadening of the chain length distribution will occur.

Random Coupling Statistics. When considering a block copolymerization, the first block should not have an influence on the growth of the second block. This is also known as the random coupling hypothesis, and Wilczek-Vera et al. have proved this to be valid by statistical analysis of their systems.[26−28] If the random coupling hypothesis is also valid in the polystyrene-*block*-polyisoprene system, this can be used to show that the type of analysis as provided in this article is valid, and the system does not suffer from the overlapping of individual isotopic patterns. According to the random coupling hypothesis, the theoretical block copolymer distribution can be reconstructed using the individual block distributions according to

$$\Gamma^{calc}(n_i, m_j) = \Gamma^i(n_i)\,\Gamma^j(m_j) \tag{7}$$

Table 3 shows the correlation coefficient (r), which has been evaluated by comparison of the experimental intensities and those calculated by eq 7, combined with the unexplained variance ($1 - r^2$). If the correlation had been perfect, one would have obtained a correlation of 1 and an unexplained variance of 0%. The obtained correlation coefficients of 0.998 combined with an unexplained variance that is less than 0.5% suggest that the random coupling theory can be successfully applied to the studied system and are therefore proof that the type of analysis as proposed in this article is valid, even when working on a complicated system where the isotopic patterns are showing overlap.

Conclusion

MALDI-ToF-MS has gained a lot of interest during the past years, although the number of articles where

the technique is used for a full copolymer characterization is still limited. In this article we have shown a method that enables complete structural analysis by analyzing MALDI-ToF-MS mass spectra for several polystyrene-*block*-polyisoprene samples. A complicating factor in this system is the overlap between isotopic patterns of individual polymeric chains. By comparison of the individual block distributions from polystyrene with the original polystyrene block, an excellent agreement was found, indicating that the isotopic overlap has a negligible influence. Furthermore, the technique was compared to ^{1}H NMR for the calculation of average copolymer composition, and a good comparison was obtained. Although this implies that ionization differences due to differences in chemical composition do not play a role in this system, this cannot be taken for granted. The results always have to be approached with caution. Finally, the individual block distributions obtained from the MALDI-ToF-MS mass spectra were subjected to random coupling statistics obtaining a correlation coefficient of 0.998, with unexplained variances less than 0.5%, which is an excellent achievement.

Appendix A

The correction factor cf'_X, for a polymeric species X, is defined as the ratio of the area under the theoretical isotopic distribution (A_{total}) and the intensity of the most intense isotope (I_{max}).

$$cf'_X = \frac{A_{total}}{I_{max}} \tag{8}$$

To obtain the relative abundances of this polymeric species X, a calculation procedure was used that is based on the theory of Yergey.[37]

In a MALDI-ToF-MS analysis it can be assumed that the time-of-flight of one single isotope, *i*, of species X, is normally distributed over time. Therefore, if the peak height (I_i) of this species has to be related to the peak area (A_i), the following equation holds:

$$A_i = I_i\sqrt{2\pi}\sigma \tag{9}$$

where σ is the half-width at half-height (hwhh) of the Gauss distribution. Since an increase of mass is accompanied by an increase of the width of an isotopic pattern, σ is mass dependent and can be expressed as a function of the resolution (expressed in g mol^{-1}) of the measurement:

$$\sigma = \frac{1}{2}\frac{m_{isotope}}{\text{resolution}} \tag{10}$$

Finally, the correction factor can be defined as a summation over all isotopes of species X:

$$cf'_X = \frac{\sum_{i=1}^{n_{isotopes}} I_i\sqrt{2\pi}\frac{1}{2}\frac{m_{isotope}}{\text{resolution}}}{I_{max}} \tag{11}$$

Although the correction factor is dependent on the resolution of a measurement, and may therefore vary from measurement to measurement, it is a constant in the expression for a specific measurement and can therefore be set to 1, resulting in the general formula:

$$cf_X = \frac{\sum_{i=1}^{n_{isotopes}} I_i\sqrt{2\pi}\frac{1}{2}m_{isotope}}{I_{max}} \quad \text{with } m_{isotope} < \text{resolution} \tag{12}$$

The obtained equation only holds when there is no overlapping between neighboring isotopes. However, as long as the evaluated masses are smaller than the resolution of the measurement, the influence of this overlapping can be neglected.

In the case of polystyrene-*block*-polyisoprene the correction factor ($cf_{i,j}$) has to be calculated for all possible combinations of styrene and isoprene monomers, e.g.

$$C(CH_3)_3[C_8H_8]_n[C_5H_8]_m-H-Ag^+ \quad \text{with } n, m = 0, 1, ..., 100$$

This correction factor can be visualized as a 3-dimensional plot as shown in Figure 7. Please note that due to the elimination of the resolution in eq 11, the correction factor results in a high value.

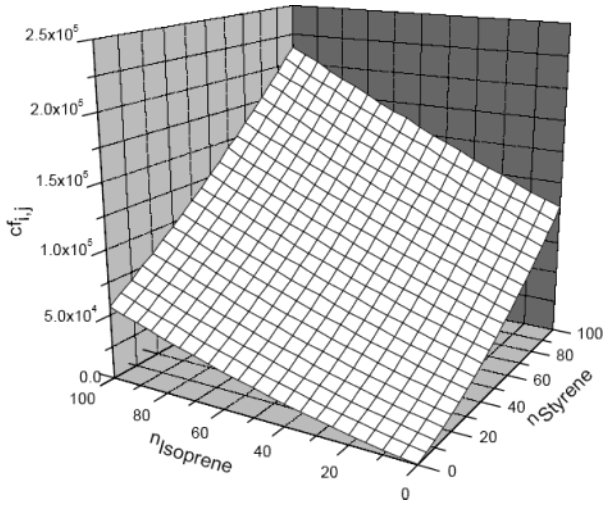

Figure 7. Three-dimensional plot for the correction factor ($cf_{i,j}$) for the system polystyrene-*block*-polyisoprene as a function of the number of monomeric units, calculated using eq 12.

Appendix B

The evaluation of the individual block properties was done by

$$P_n = \frac{\sum_i n_i\Gamma^i(n_i)}{\sum_i \Gamma^i(n_i)} \tag{13}$$

$$P_w = \frac{\sum_i n_i^2\Gamma^i(n_i)}{\sum_i n_i\Gamma^i(n_i)} \tag{14}$$

$$PDI = \frac{P_w}{P_n} \tag{15}$$

Polymer composition of monomer *i*:

$$F_i = \frac{\sum_{i=1}^{n}\sum_{j=1}^{n} n_i I_{(i,j)} c f_{i,j}}{\sum_{i=1}^{n}\sum_{j=1}^{n} (n_i + m_j) I_{(i,j)} c f_{i,j}} \qquad (16)$$

Supporting Information Available: MALDI-ToF-MS mass spectra for the system polystyrene-*block*-polyisoprene after approximately 25% and 75% conversion of the isoprene monomer; furthermore, an example illustrating the effect of multiple peak assignments for copolymer mass spectra. This material is available free of charge via the Internet at http://pubs.acs.org.

References and Notes

(1) Montaudo, M. S. *Polymer* **2002**, *43*, 1587−1597.
(2) Montaudo, M. S. *Macromolecules* **2001**, *34*, 2792−2797.
(3) Servaty, S.; Koehler, W.; Meyer, W. H.; Rosenauer, C.; Spickermann, J.; Raeder, H. J.; Wegner, G.; Weier, A. *Macromolecules* **1998**, *31*, 2468−2474.
(4) Van Doremaele, G. H. J.; Geerts, F. H. J. M.; Aan de Meulen, L. J.; German, A. L. *Polymer* **1992**, *33*, 1512−1518.
(5) Van Doremaele, G. H. J.; Tacx, J. C. J. F.; Ammerdorffer, J. L. *J. Planar Chromatogr.—Mod. TLC* **1991**, *4* (Jan−Feb), 46−51.
(6) Adrian, J.; Esser, E.; Hellmann, G.; Pasch, H. *Polymer* **1999**, *41*, 2439−2449.
(7) Siewing, A.; Schierholz, J.; Braun, D.; Hellmann, G.; Pasch, H. *Macromol. Chem. Phys.* **2001**, *202*, 2890−2894.
(8) Pasch, H.; Mequanint, K.; Adrian, J. *e-Polym.* **2002**, *5*.
(9) van der Horst, A.; Schoenmakers, P. J. *J. Chromatogr., A* **2003**, *1000*, 693−709.
(10) Graef, S. M.; van Zyl, A. J. P.; Sanderson, R. D.; Klumperman, B.; Pasch, H. *J. Appl. Polym. Sci.* **2003**, *88*, 2530−2538.
(11) Pasch, H.; Kilz, P. *GIT Labor-Fachzeitschrift* **1999**, *43*, 239−240.
(12) Siewing, A.; Lahn, B.; Braun, D.; Pasch, H. *J. Polym. Sci., Part A: Polym. Chem.* **2003**, *41*, 3143−3148.
(13) Adrian, J.; Braun, D.; Pasch, H. *Angew. Makromol. Chem.* **1999**, *267*, 82−88.
(14) Kilz, P.; Krueger, R. P.; Much, H.; Schulz, G. *Adv. Chem. Ser.* **1995**, *247*, 223−241.
(15) Lou, X.; Dongen, J. L. J. v.; Meijer, E. W. *J. Chromatogr., A* **2000**, *896*, 19−30.
(16) Lou, X.; Dongen, J. L. J. v. *J. Mass Spectrom.* **2000**, *35*, 1308−1312.
(17) Montaudo, M. S.; Puglisi, C.; Samperi, F.; Montaudo, G. *Macromolecules* **1998**, *31*, 3839−3845.
(18) Mayer-Posner, F. J.; Kaminski, H.; Sauerland, V.; Ndoni, S.; Badsberg Petersen, W.; Hivdt, S.; Kingshott, P. *Abstracts of Papers, 225th ACS National Meeting*, 2003.
(19) Murgasova, R.; Brantley, E. L.; Hercules, D. M.; Nefzger, H. *Macromolecules* **2002**, *35*, 8338−8345.
(20) Esser, E.; Keil, C.; Braun, D.; Montag, P.; Pasch, H. *Polymer* **2000**, *41*, 4039−4046.
(21) Tatro, S. R.; Baker, G. R.; Fleming, R.; Harmon, J. P. *Polymer* **2002**, *43*, 2329−2335.
(22) Lou, X.; van Dongen, J. L. J.; Janssen, H. M.; Lange, R. F. M. *J. Chromatogr., A* **2002**, *976*, 145−154.
(23) Puglisi, C.; Samperi, F.; Carroccio, S.; Montaudo, G. *Rapid Commun. Mass Spectrom.* **1999**, *13*, 2260−2267.
(24) Puglisi, C.; Samperi, F.; Carroccio, S.; Montaudo, G. *Rapid Commun. Mass Spectrom.* **1999**, *13*, 2268−2277.
(25) Philipsen, H. J. A.; Wubbe, F. P. C.; Klumperman, B.; German, A. L. *J. Appl. Polym. Sci.* **1999**, *72*, 183−201.
(26) Wilczek-Vera, G.; Yu, Y.; Waddell, K.; Danis, P.; Eisenberg, A. *Rapid Commun. Mass Spectrom.* **1999**, *13*, 764−777.
(27) Wilczek-Vera, G.; Yu, Y.; Waddell, K.; Danis, P. O.; Eisenberg, A. *Macromolecules* **1999**, *32*, 2180−2187.
(28) Wilczek-Vera, G.; Danis, P. O.; Eisenberg, A. *Macromolecules* **1996**, *29*, 4036−4044.
(29) Suddaby, K. G.; Hunt, K. H.; Haddleton, D. M. *Macromolecules* **1996**, *29*, 8642−8649.
(30) van Rooij, G. J.; Duursma, M. C.; de Koster, C. G.; Heeren, R. M. A.; Boon, J. J.; Schuyl, P. J. W.; van der Hage, E. R. E. *Anal. Chem.* **1998**, *70*, 843−850.
(31) Wu, S.; Percy, J.; Hsu, S. L.; Kaltashov, I. A.; Stidham, H. D. *Cellul. Polym.* **2003**, *22*, 23−42.
(32) Ulmer, L.; Mattay, J.; Torres-Garcia, H. G.; Luftmann, H. *Eur. J. Mass. Spectrom.* **2000**, *6*, 49−52.
(33) Wallace, W. E.; Guttman, C. M. *J. Res. Natl. Inst. Stand. Technol.* **2002**, *107*, 1−17.
(34) A computer program implementing the principles outlined in this article is available from the authors. Please note that the computer program only works in conjunction with the DataExplorer software from Applied Biosystems.
(35) McEwen, C. N.; Jackson, C.; Larsen, B. S. *Int. J. Mass Spectrom. Ion Proc.* **1997**, *160*, 387−394.
(36) Hsieh, H. L.; Quirk, R. P. *Anionic Polymerization: Principles and Practical Applications;* Dekker: New York, 1996.
(37) Yergey, J. A. *Int. J. Mass Spectrom. Ion Phys.* **1983**, *52*, 337−349.

MA049471M